



Pergamon

Modulation of the Skeletal Muscle Ca^{2+} Release Channel/Ryanodine Receptor by Adenosine and Its Metabolites: A Structure–Activity Approach

Armando Butanda-Ochoa,^a Germund Höjer^b and Mauricio Díaz-Muñoz^{a,*}

^a*Departamento de Neurobiología Celular y Molecular, Instituto de Neurobiología, UNAM, Juriquilla Querétaro 76001, Apdo. Postal 1-1141, Mexico*

^b*Departamento de Física y Química Teórica, Facultad de Química, UNAM, Cd. Universitaria, 04510, Mexico D.F.*

Received 1 August 2002; accepted 11 October 2002

Abstract—Activation of ryanodine receptor (RyR) from skeletal muscle sarcoplasmic reticulum by adenosine and adenosine's metabolites was studied. The purines tested increased the [^3H]-ryanodine binding as follows: xanthine > adenosine > adenine > inosine \geq uric acid > hypoxanthine. The enhanced [^3H]-ryanodine binding did not involve change in the RyR- Ca^{2+} sensitivity and was due mainly to lower values in the affinity constant (K_d) that corresponded with an increase in the association rate constant (K_{+1}). [^3H]-ryanodine maximum binding (B_{max}) was much less affected. Adenosine and inosine effects were dependent on the presence β -glycosidic bond within the ribose ring, since the combination of adenine or hypoxanthine with ribose was not able to emulate the nucleosides' original activation. Competition experiments with AMP-PCP, a non-hydrolyzable analogue of ATP, evidenced a nucleotide's inhibitory influence on the adenosine and xanthine activation of the RyR. As a result of a Quantitative Structure–Activity Relationship (QSAR) study, we found a significant correlation between the modulation by adenosine and its metabolites on RyR activity and the components of their calculated dipole moment vector. Our results show that the ribose moiety and the dipole moment vector could be factors that make possible the modulation of the RyR activity by adenosine and its metabolites.

© 2003 Elsevier Science Ltd. All rights reserved.

Introduction

The ryanodine receptor (RyR) from the sarcoplasmic reticulum (SR) plays a key role in the excitation–contraction coupling at the triad junction acting as a calcium release channel. The RyR type 1 is the major isoform in the skeletal muscle, and it has been described as a homotetrameric receptor-channel of high molecular weight (~ 565 kDa per monomer)¹ with allosteric properties that can be modulated by a great variety of agents, including ATP and caffeine.²

Regulation of RyR by purines is not simple, since different modes of activation have been postulated for these purines: The adenine nucleotide stimulates the [^3H]-ryanodine binding affinity and enhances the open probability of the channel, in a calcium-independent manner, whereas caffeine activates the RyR by enhancing

its affinity to calcium.^{3–5} The different effects on the activity of RyR have suggested that this receptor-channel has separate (but mutually interactive) binding sites for each of these purines.⁶

Besides the well studied effects of ATP and caffeine on the RyR activity, very few experimental observations exist about the role of other purines as potential modulators of the RyR.^{7,8} This lack of information is more evident when purines of physiological significance are considered.

This study describes the effect of adenosine and its metabolites (adenine, inosine, hypoxanthine, xanthine and uric acid) on the [^3H]-ryanodine binding of the RyR from rabbit sarcoplasmic reticulum. It provides evidence that at least two molecular parameters are involved in the RyR modulation by these purines: the dipole moment vector and the presence of the ribose ring. Finally, it is demonstrated that the activation of RyR by adenosine and xanthine is modulated by AMP-PCP.

*Corresponding author. Tel/fax: +52-5-6-23-4035; e-mail: mdiaz@calli.cnbi.unam.mx

Results

Modulation of RyR by adenosine and its metabolites

[³H]-Ryanodine binding assay can be used as a probe of the functional state of the RyR channel.^{6,9} According to these reports, experimental conditions that increase the activity of the RyR lead to an increase of [³H]-ryanodine binding, whereas the RyR inhibition is associated to a diminution in the bound [³H]-ryanodine. Hence, our first approach to assess the modulating action of adenosine and its metabolites on the activity of the skeletal muscle RyR was to elaborate [³H]-ryanodine binding dose-response curves for adenosine and its metabolites.

Figure 1 shows the pattern of activation of [³H]-ryanodine binding associated to the presence of adenosine (Panel A), inosine (Panel B), hypoxanthine (Panel C), xanthine (Panel D) and uric acid (Panel E). The dose-response curves were normalized with respect to the control condition (no purine addition). RyR was activated differentially by all the purines tested, but in each case the pattern of activation was neither hyperbolic nor sigmoid. Distinct to ATP which activates RyR at mM range,³ adenosine and its metabolites increased the [³H]-ryanodine binding acting in the range of 1–10 nM (adenosine, inosine, xanthine and uric acid) or low μ M (hypoxanthine) concentrations.

Adenosine reached its maximal activation (4.40 ± 0.46 times over control) at 1 nM. When adenosine concentration was increased into the μ M–mM range, its activation diminished to half of the maximal response.

Inosine showed a maximal activation (2.60 ± 0.35 times over control) at 10 nM. At higher concentrations, its activation decreased near the control level.

Hypoxanthine was the weakest activating purine tested. It only caused a modest activation of 1.70 ± 0.18 times over control at 10 μ M. In contrast, xanthine was the most effective reaching a maximal [³H]-ryanodine binding of 6.20 ± 0.95 times over control at 10 nM. As with the inosine effect, the xanthine activation decreased gradually at higher concentrations.

The dose-response curve of uric acid exhibited a pattern similar to xanthine. However, uric acid was less potent and its maximal activation at 10 nM (2.00 ± 0.18 times over control) was 66% minor than the activation promoted by xanthine.

Role of ribose ring

Distinctively to the rest of the purines tested, adenosine and inosine present a ribose moiety joined through a β -glycosidic bond to the purine ring. To investigate whether or not the activation of RyR by optimal concentrations of adenosine (1 nM) and inosine (10 nM) was dependent of the ribose ring within their structure, the [³H]-ryanodine binding assay was done with the next protocols: For adenosine: (1) adenosine (purine with the sugar), (2) adenine (only the purine), (3) ribose (only the sugar), and (4) the mixture of adenine and ribose. For

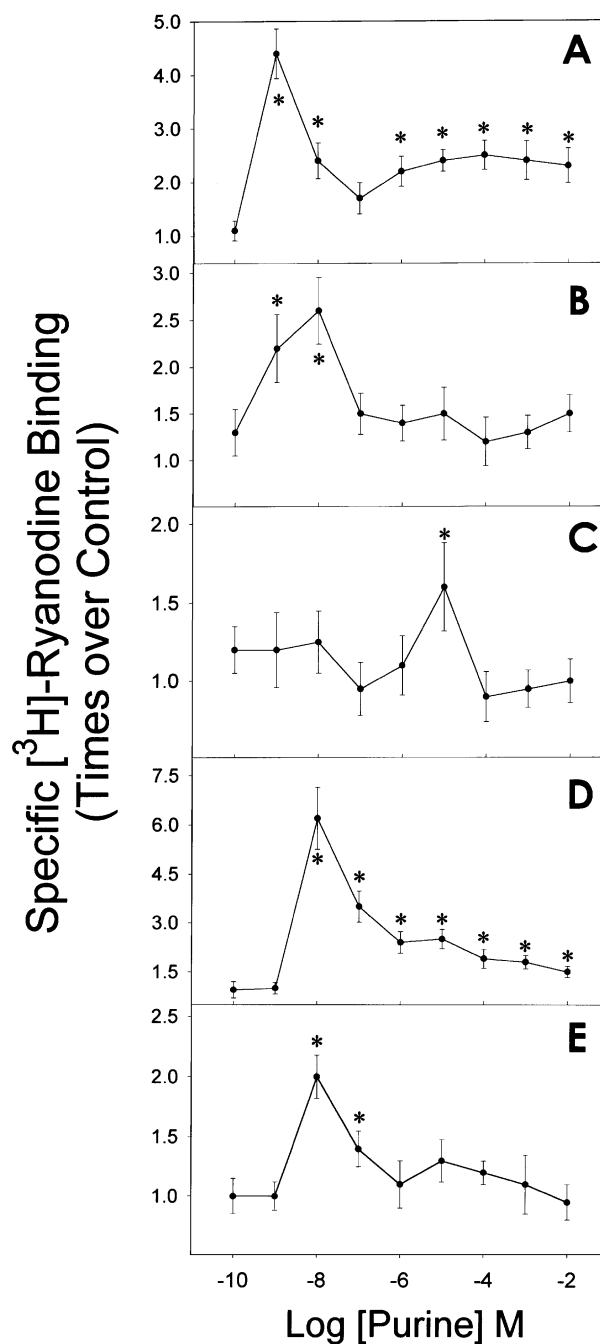


Figure 1. Effect of adenosine and its metabolites on [³H]-ryanodine binding. Each dose-response curve was normalized with respect to control condition (1.00 ± 0.08 pmol/mg protein): (A) adenosine, (B) inosine, (C) hypoxanthine, (D) xanthine and (E) uric acid. Heavy SR membranes (10 μ g) were incubated for 12–14 h in assay buffer (see Experimental) containing 6 nM [³H]-ryanodine and 100 μ M of Ca^{2+} . Data are means \pm SEM of at least four independent experiments. (*) indicates statistical significance versus control. α set at $p < 0.05$.

inosine: (1) inosine (purine with the sugar), (2) hypoxanthine (only the purine), (3) ribose (only the sugar), and (4) the mixture of hypoxanthine and ribose. Figure 2 shows that the activation of RyR by adenosine and inosine was dependent on the presence of the ribose within their structure, since neither the sole purine (adenine or hypoxanthine), nor the sugar or the combination of purine and sugar, were able to increase the [³H]-ryanodine binding.

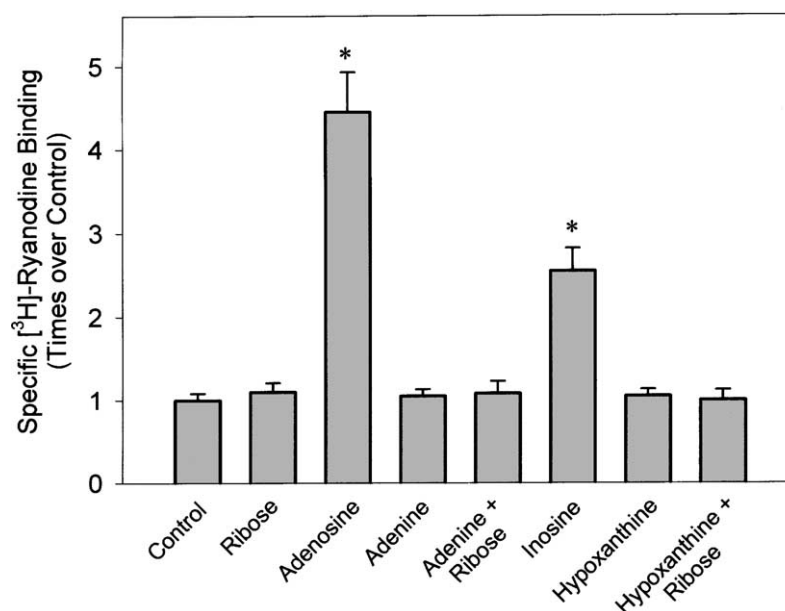


Figure 2. Role of ribose ring in the activation of the RyR by adenosine and inosine. [^3H]-Ryanodine binding was done in the presence of the nucleosides (adenosine 1 nM or inosine 10 nM), the purine bases (adenine 1 nM or hypoxanthine 10 nM), ribose (1 or 10 nM) and the mixture of purine bases and ribose. The result corresponding to ribose is an average of the two concentrations used, since no difference between them was observed. Heavy SR membranes (10 μg) were incubated for 12–14 h in assay buffer (see Experimental) containing 6 nM [^3H]-ryanodine and 100 μM of Ca^{2+} . Data are means \pm SEM of at least four independent experiments. * indicates statistical significance versus control. α set at $p < 0.05$.

RyR binding constants

To discriminate if the enhancement in [^3H]-ryanodine binding in presence of adenosine and its metabolites was due to an increase in the [^3H]-ryanodine affinity (K_d) or in the number of binding sites (B_{max}), Scatchard analysis was applied to [^3H]-ryanodine saturation isotherms for each purine tested at their most effective concentration. Values of K_d , B_{max} , and Hill coefficient of each experimental condition are shown in Table 1, which also includes the [^3H]-ryanodine binding parameters in presence of adenine assessed at 1 mM. This concentration corresponds to the maximum response obtained by other groups using ^{45}Ca release and electrophysiological studies.^{10,11} Adenine was able to increase 2.9 ± 0.01 times over control the [^3H]-ryanodine binding. The [^3H]-ryanodine binding parameters obtained in presence of adenine were later used in the QSAR analysis.

The [^3H]-ryanodine binding values in control conditions were similar to those previously reported ($K_d = 8.22 \pm 1.16$, $B_{\text{max}} = 14.48 \pm 2.73$ and Hill coefficient = 1.05 ± 0.12).^{9,12} We were able to reproduce the increase

in [^3H]-ryanodine binding promoted by AMP-PCP that involves a significant enhance in the [^3H]-ryanodine affinity, ($K_d = 1.38 \pm 0.26$ nM), a modest augmentation in the number of [^3H]-ryanodine binding sites ($B_{\text{max}} = 17.41 \pm 2.98$ pmol/mg protein) and a significant cooperativity (Hill coefficient = 1.89 ± 0.26).^{6,10} The binding constants in the presence of adenosine and its metabolites were similar, if not totally, to those promoted by AMP-PCP. The action of adenosine, adenine, inosine, hypoxanthine, xanthine and uric acid was to activate the [^3H]-ryanodine binding primarily by decreasing the K_d (range from 1.39 nM for xanthine to 2.96 nM for hypoxanthine), and increasing only moderately the B_{max} (range from 16.73 pmol/mg protein for hypoxanthine to 19.88 pmol/mg protein for xanthine). However, differently to the effect of AMP-PCP, adenosine and its metabolites did not change the cooperativity of the saturation isotherms, being in all the cases the Hill coefficient close to 1.

We further explored if the increase in [^3H]-ryanodine affinity promoted by adenosine and its metabolites was

Table 1. [^3H]-Ryanodine constants in presence of activator concentrations of adenosine and adenosine metabolites

Modulator	K_d (nM)	B_{max} (pmol/mg protein)	Hill coefficient	K_{+1} ($\mu\text{M}^{-1} \text{min}^{-1}$)
Control	8.22 ± 1.16	14.48 ± 2.73	1.05 ± 0.12	0.38 ± 0.05
+ Adenosine (1 nM)	$1.45 \pm 0.25^*$	19.37 ± 2.99	1.04 ± 0.15	$1.52 \pm 0.23^*$
+ Inosine (10 nM)	$2.00 \pm 0.22^*$	17.45 ± 2.60	1.10 ± 0.09	$1.10 \pm 0.20^*$
+ Hypoxanthine (10 μM)	$2.96 \pm 0.29^*$	16.73 ± 2.21	0.95 ± 0.14	$0.74 \pm 0.09^*$
+ Xanthine (10 nM)	$1.39 \pm 0.19^*$	19.88 ± 2.54	0.99 ± 0.17	$1.58 \pm 0.28^*$
+ Uric acid (10 nM)	$2.15 \pm 0.27^*$	18.43 ± 3.02	0.98 ± 0.20	$1.02 \pm 0.17^*$
+ AMP-PCP (1 mM)	$1.38 \pm 0.26^*$	17.41 ± 2.98	$1.89 \pm 0.26^*$	$1.59 \pm 0.24^*$
+ Adenine (1 mM)	$1.96 \pm 0.18^*$	18.32 ± 3.39	1.02 ± 0.21	$1.13 \pm 0.21^*$

Experimental conditions were described in the Experimental. K_d and B_{max} were obtained directly from binding isotherms ($r_{\text{mean}} = 0.9975$), the Hill coefficients by linear regression analysis ($r_{\text{mean}} = 0.9424$). The association rate constants (K_{+1}) were derived from the slope of association plots ($r_{\text{mean}} = 0.9694$). Data are means \pm SEM of at least four independent experiments, α set at $p < 0.05$.

due to an enhancement in the association rate constant (K_{+1}). The results are also shown in Table 1. Again, adenosine and its metabolites had a similar action to the one reported for AMP-PCP: they increased significantly the association rate constant of the [3 H]-ryanodine binding assay. The mechanism explaining the augmentation in affinity of [3 H]-ryanodine by adenosine and its metabolites seems coincident to the one associated to the action of ATP.

Calcium dependence

To further explore the molecular mechanisms by which adenosine and its metabolites activate the skeletal muscle RyR, the Ca^{2+} dependence to stimulate [3 H]-ryanodine binding was tested. Increment in free [Ca^{2+}] produced a bell-shaped curve in [3 H]-ryanodine binding under control conditions, with an optimal binding at micromolar range (Fig. 3). In the presence of 20 mM caffeine, it was observed a shift in the curve towards lower Ca^{2+} concentrations, with a clear increase in the [3 H]-ryanodine binding at 1 nM of free Ca^{2+} confirming previous reports.^{2,13} In contrast, 1 mM AMP-PCP increased the total amount of [3 H]-ryanodine binding, without a significant influence in the Ca^{2+} sensitivity.

Figure 3 shows that, similarly to AMP-PCP, and in contrast to caffeine, adenosine and its metabolites also enhanced the total amount of [3 H]-ryanodine binding, without any effect in the Ca^{2+} sensitivity of the RyR. The Hill analysis applied to the activation and inactivation segments of the calcium-dependence curves, showed no difference between the control condition and the responses elicited by adenosine and its metabolites (data not shown).

Influence of AMP-PCP on activation of RyR by adenosine and xanthine

Given the lack of effect of adenosine and its metabolites in the calcium sensitivity of [3 H]-ryanodine binding, and the coincidence between AMP-PCP and the purines tested in increasing the [3 H]-ryanodine binding by enhancing the association constant rate (K_{+1}), we hypothesized that adenosine and its metabolites were more predisposed to interact with the ATP binding site in the RyR, more than with the caffeine binding site. Figure 4 shows competition experiments aimed to explore the influence of AMP-PCP on [3 H]-ryanodine binding enhanced by adenosine and xanthine (Panel A and B), as well as the effect of adenosine and xanthine on the [3 H]-ryanodine binding promoted by AMP-PCP (Panel C). Adenosine and xanthine were selected for these experiments since they were the more effective purines to stimulate the activation of RyR (see Fig. 1).

Figure 4, in Panels A and B, shows that AMP-PCP was able to counteract the optimal stimulation of [3 H]-ryanodine binding elicited by 1 nM adenosine and 10 nM xanthine. A remarkable aspect of this inhibitor action of AMP-PCP was that occurred at nM– μ M concentrations of the nucleotide, range in which AMP-PCP does not promote any activation of RyR by itself. The IC_{50} values showed that adenosine activation of [3 H]-ryanodine binding was less susceptible to be inhibited by AMP-PCP than xanthine ($\text{IC}_{50} = 0.706 \pm 0.058 \mu\text{M}$, for adenosine and $\text{IC}_{50} 0.063 \pm 0.052 \mu\text{M}$, for xanthine, $n = 4$).

Figure 4, Panel C, shows that neither adenosine nor xanthine at their optimal stimulatory concentrations (1 and 10 nM, respectively) were effective to change the

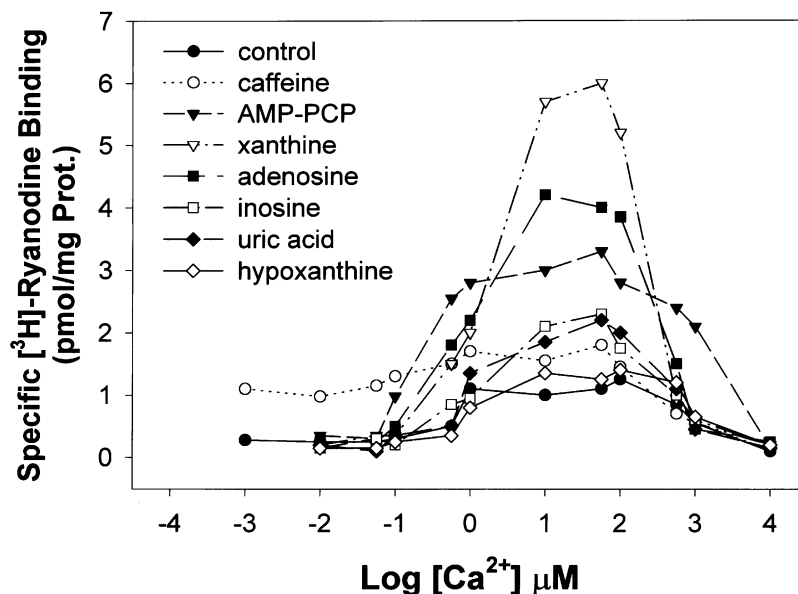


Figure 3. Calcium dependence of the action of adenosine and its metabolites on [3 H]-ryanodine binding. Experiments were done using the most effective concentrations of adenosine and its metabolites: 1 nM adenosine, 10 nM inosine, 10 μM hypoxanthine, 10 nM xanthine, 10 nM uric acid. To compare with actions already reported, 1 mM AMP-PCP and 20 mM caffeine were also included. Heavy SR membranes (10 μg) were incubated for 12–14 h in assay buffer (see Experimental) containing 6 nM [3 H]-ryanodine. Data are means of at least four independent experiments. SEM are not shown to clarify the figure, and varied between 7 and 22% of the mean values.

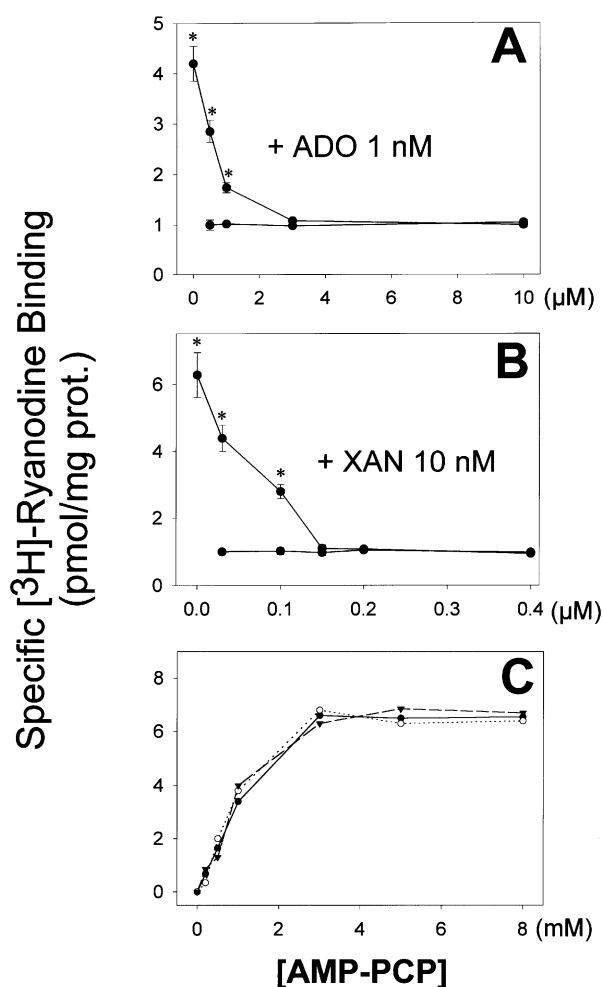


Figure 4. AMP-PCP blocks the increase in [^3H]-ryanodine binding promoted by adenosine and xanthine. Panels A and B are competition experiments that show the influence of AMP-PCP, at nM– μM range, on [^3H]-ryanodine binding enhanced by 1 nM adenosine and 10 nM xanthine, respectively. Adenosine and xanthine are depicted as ADO and XAN, respectively. In Panel C, the effect of 1 nM adenosine and 10 nM xanthine on the [^3H]-ryanodine binding promoted by AMP-PCP at μM –mM range is shown. Heavy SR membranes (10 μg) were incubated for 12–14 h in assay buffer (see Experimental) containing 6 nM [^3H]-ryanodine and 100 μM of Ca^{2+} . Data are means \pm SEM of at least four independent experiments. * indicates statistical significance versus control. α set at $p < 0.05$. Where not shown, error bars are smaller than symbols.

hyperbolic stimulatory pattern of [^3H]-ryanodine binding elicited by mM concentrations of AMP-PCP. The cooperativity promoted by AMP-PCP in the [^3H]-ryanodine binding was not affected either (data not shown).

Dipole moment calculations

The dipole moment vector (μ) was calculated to gain comprehension about the mechanism by which adenosine and its metabolites activate skeletal muscle RyR. To represent μ graphically, we adopted the standard chemical convention with the vector pointing from the positive to the negative charge.¹⁴ The μ orientation and magnitude of each purine are shown in Table 2. The origin of the coordinate system was fixed at the C4 of each purine ring, N9 defines the positive x -axis, C8 is placed in the first quadrant of the xy -plane, and the

Table 2. Calculated dipole moment vector (μ) 3-D components of adenosine and its metabolites

Metabolite	Binding (times over control)	x	y	z	Polarity (debyes)
Xanthine	6.20	5.92	−4.87	0.00	7.66
Adenosine (syn)	4.40	2.85	2.20	1.58	3.93
Adenine	2.90	2.38	0.69	−0.56	2.54
Inosine (syn)	2.60	−0.74	−3.98	1.57	4.34
Uric acid	2.00	0.93	−3.07	0.00	3.20
Hypoxanthine	1.70	0.92	−5.53	0.00	5.60

The origin of the coordinate system was fixed at C4 of the purine ring, N9 defines the positive x -axis, and C8 is placed in the first quadrant of the xy -plane, and the positive z -axis points perpendicularly up from the xy -plane (paper plane). The calculation algorithm follows the physical definition of the dipole moment (components reported in this table). In the graphical representation shown in Figure 5, the standard chemical convention is used, the dipole vector points from the positive to the negative charge. As a result, a vector with calculated positive z -component points into the paper, and a vector with calculated negative z -component points out of the paper. All the structures were calculated according to their predominating tautomeric (keto-enol) form at pH 7.

positive z -axis points perpendicularly up from the xy -plane (paper plane). Only the syn conformers of adenosine and inosine were considered, since they are the predominant forms of these molecules in aqueous solution.^{14–18}

Figure 5 shows the graphic representation of μ for adenosine and its metabolites. Adenosine and xanthine, the most effective purines in increasing [^3H]-ryanodine binding, presented xy -components of their μ towards the region between C6 and N3. The z -component of μ in xanthine was zero whereas for adenosine was positive (Table 2). In adenine, which was less efficient than adenosine at nM range to activate the RyR, the in-plane component of μ was directed to the same region as xanthine and adenosine (C6 and N3), but due the pyramidal amino group in C6, it presents a negative z -component.

The in-plane components of the dipole vectors in the less effective purines, hypoxanthine, inosine and uric acid, were oriented towards the region limited by C5, N7 and C8. The only one of these purines with a positive z -component was inosine (Table 2).

A positive value of the z -component in the nucleosides, adenosine and inosine, correlated with the presence of the ribose ring in these molecules. The activation of the nucleosides in the [^3H]-ryanodine binding was more efficient than their corresponding sugar-less bases, adenine and hypoxanthine, which presented a negative or a null z -component, respectively.

To explore a potential association between the effectiveness of [^3H]-ryanodine binding modulation by adenosine and its metabolites and the components of their dipole moment vector, a Quantitative Structure–Activity Relationship (QSAR) was performed based in the μ values listed in Table 2 and the value of maximum level of activation on [^3H]-ryanodine binding depicted in Figure 1. The QSAR revealed a significant correlation

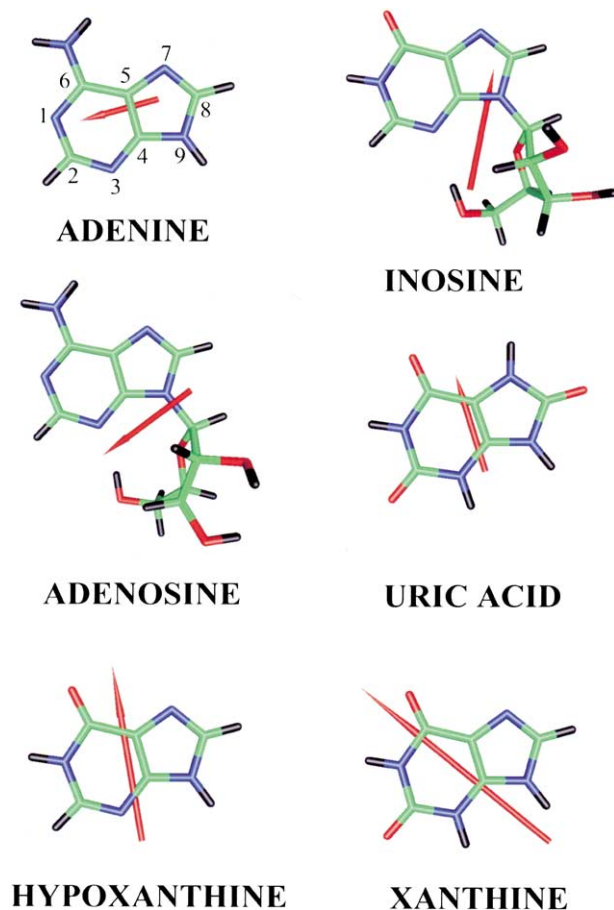


Figure 5. Molecular structures and dipole moment vector (μ) of adenosine and its catabolites. Predominant keto tautomers at pH 7 were calculated by ab initio methods (see Experimental). The origin of the coordinate system was fixed at C4 of the purine ring, N9 defines the positive x -axis, and C8 is placed in the first quadrant of the xy -plane, and the positive z -axis points perpendicularly up from the xy -plane (paper plane). The numbers correspond to the purine atoms. Only the syn conformers of adenosine and inosine were taken into account, since they are the favored conformation of nucleosides in aqueous solution.

between the x - and z -components and the maximal value of activation of $[^3\text{H}]$ -ryanodine binding. The results are summarized in the linear equation:

$$y = 0.763x + 0.810z + 1.391$$

where:

y = maximal response	$r^2 = 0.95$
x = x -component of μ	$r^2_{\text{adj}} = 0.92$ (six observations)
z = z -component of μ	$F = 28.79$ (significant at the 1.1% level)

r^2_{adj} , the squared adjusted linear correlation coefficient, is a more convenient and stricter parameter to validate significant results in situations that involve a not very large number of observations.¹⁹

Exclusively the syn conformers of adenosine and inosine were considered for the QSAR analysis. ATP, which modulates the RyR through its deprotonated Mg^{2+} -complex,²⁰ was excluded since the QSAR analysis was based solely on the non-ionic form of the purines, which is the preponderant form of adenosine and its metabolites at physiological pH.^{21,22}

Discussion

Adenosine and its metabolites as modulators for skeletal muscle ryanodine receptor

It is well known that RyRs are modulated by purines acting at mM concentrations such as ATP and caffeine.^{2,6,23} Here, for the first time, we report that purines such as adenosine and its metabolites are able to perform a modulating role but at nM– μM range. The increase in $[^3\text{H}]$ -ryanodine binding elicited by adenosine and its metabolites did not show a simple pattern (Fig. 1). The existence in all cases of a maximum in the RyR activation, strongly suggests the presence of purine recognition sites with high and low affinity sites, for $[^3\text{H}]$ -ryanodine binding activation and inhibition, respectively.

The importance of the ribose moiety in the effect of adenosine and inosine was evident when the action of these nucleosides on $[^3\text{H}]$ -ryanodine binding were compared with the effect promoted by adenine and hypoxanthine, and also when they were mixed with ribose (Fig. 2). These data indicate that the presence within the molecule of a β -glycosidic bond is necessary to elicit a full response. It is probable that the β -glycosidic bond between the purine and the ribose ring permits the correct orientation of both moieties to interact in a more effective way with the RyR. The relevance of the ribose moiety could be extended to other kind of interactions since the brain RyR appears to require the oxidation of the ribose moiety to achieve a higher activation of $[^3\text{H}]$ -ryanodine binding.⁷

Adenosine and its metabolites increased $[^3\text{H}]$ -ryanodine binding without changing the calcium sensitivity of RyR (Fig. 3). This result makes the effect of adenosine and its metabolites different to that of caffeine. We do not know if adenosine and its metabolites are recognized at the same binding sites as AMP-PCP in the RyR structure. However, as adenosine and its metabolites increased the $[^3\text{H}]$ -ryanodine binding affinity through the same mechanism as the nucleotide (enhancing the association rate constant, Table 1), it is possible that adenosine and its metabolites could be recognizing the same binding sites that AMP-PCP (ATP). Another possibility is the existence of separate, but interacting, binding sites for ATP and adenosine and its metabolites. Data in Figure 4 show that AMP-PCP in μM and sub- μM concentrations inhibits the increase of $[^3\text{H}]$ -ryanodine binding promoted by adenosine and xanthine. The action exerted by AMP-PCP is unexpected since no effect on RyR has been reported for AMP-PCP or ATP in concentrations below the mM range. Two possible interpretations of this result are: (1) AMP-PCP competes directly with adenosine and xanthine at their binding sites, or (2) there is a high affinity binding site for AMP-PCP that is modulating the affinity of adenosine and xanthine binding sites. In both possibilities the molecular structure of the purine modulator is a relevant factor since the AMP-PCP was 11 times more effective to inhibit the increase of $[^3\text{H}]$ -ryanodine binding promoted by xanthine than the one promoted by adenosine. Further experiments should be made to investigate this point.

Eight ATP binding domains (Gly-loops) are found in each monomer of RyR type 1 according to the primary structure of this Ca^{2+} release channel.²⁴ The crystallized structure of this motif was resolved for the protein kinase A,²⁵ but nothing is known about the accessibility, folding or 3-D-structure of these ATP binding domains in the RyR type 1. Shoshan-Barmatz's group has reported that skeletal muscle²⁶ and brain²⁷ RyR bind the ATP analogue *O*-(4-benzoyl)benzoyl ATP with a stoichiometry of 1:1. This number is in contrast with the potential 32 different sites for ATP that are present in the amino acid sequence of the RyR. This group reported that adenosine was able to antagonize the binding of the ATP analogue to the skeletal muscle RyR, suggesting that both molecules could be bound to the same site.²⁴

Using a comparative molecular field analysis (COMFA), Chan et al. reported that among the structural factors determining the ability of ATP to activate the cardiac RyR, is the large electrostatic field in the vicinity of the ionized phosphate groups.¹¹ According to these authors, adenosine tested at mM concentration activates the cardiac RyR with lower efficacy than ATP since the strength of the field is reduced by the absence of the phosphate groups. They also observed that steric interactions between the cardiac RyR and the α -phosphate and ribose moieties are correlated with the open probability of the receptor. For several reasons, we cannot compare directly the results obtained by Chan et al. with the findings of this work: (1) They did not use skeletal muscle RyR as subject for their study, (2) all the purine tested were used in mM range, and (3) unitary activity for channels incorporated in bilayers was used to determine the RyR activity. However, it is interesting that our results confirm the discrimination between the caffeine and adenine nucleotide sites in skeletal muscle RyR by adenosine reported previously in cardiac RyR.²⁸

Role of the dipole moment vector in the modulation of the RyR by adenosine and its metabolites

The way in which a molecule with ligand properties, orientates in the electric field of a receptor binding site, is a fundamental factor that governs the recognition between these two entities. The QSAR analysis strongly suggests the importance of the *x*- and *z*-components of the dipole moment vector in the modulatory action of adenosine and its metabolites on skeletal muscle RyR. These μ components could be related to the optimal orientation of the purine modulators to achieve the RyR activation. The results imply that the μ vector of the most effective modulators of [³H]-ryanodine binding such as adenosine, xanthine, inosine and adenine, is mainly directed towards the purine ring, but also with an important component orientated out of the purine plane.

The activation of [³H]-ryanodine binding by adenosine and its metabolites, depends on all components of the dipole moment vector. A change in the value of one of these components may be fully or partially compensated by a change in other different component. For example, the large value of the *x*-component in xanthine, the most effective purine to increase [³H]-ryanodine bind-

ing, compensates the complete lack of a *z*-component. In comparison, the *x*-component of adenosine is smaller ~ 3 debyes compared to the one of xanthine. However, an increment of ~ 1.6 debyes in the positive *z*-component of adenosine compensates the reduction in the *x*-component, resulting in that the maximal [³H]-ryanodine binding promoted by adenosine was only 29% smaller than the response of xanthine. Adenine, as adenosine, presented a reduction in its *x*-component (~ 3.5 debyes), but because of a negative value for its *z*-component, its maximal [³H]-ryanodine binding was 50% lower. For hypoxanthine and uric acid, the smaller values of their *x*-components did not compensate the lack of a *z*-component, and their maximal [³H]-ryanodine binding were only 30% of that promoted by xanthine. However, inosine also with an unfavorable *x*-component presents a compensating positive *z*-component, and its maximal [³H]-ryanodine binding was 24 and 31% higher than the ones of hypoxanthine and uric acid, respectively.

The ribose ring in the nucleosides, adenosine and inosine, is important to confer a positive value to the *z*-component of the dipolar moment vector (Table 2). However, it also could be involved in some other interactions (i.e., through its $-\text{OH}$ groups) which may enhance the activation of the RyR. This is coincident with the fact that the alteration of the ribose ring, that is oxidation in diadenosine polyphosphates derivatives, produced a higher activation of the cerebral RyR than the non oxidized derivatives.⁷

In summary, adenosine and its metabolites are purine derivatives that positively stimulates the [³H]-ryanodine binding and therefore the activity of the skeletal muscle RyR. This activation correlated significantly with the *x*- and *z*-components of the calculated dipole moment vector, suggesting that the purine orientation in the electric field at the binding site(s) is a feature involved in the optimal activation of the RyR by these purine derivatives. The results are also consistent with the idea that the RyR binding sites for adenosine and its metabolites could be the same as those for ATP.

Experimental

Materials

Adenosine, adenine, inosine, hypoxanthine, xanthine, uric acid, caffeine and EGTA were obtained from Sigma Chemical Co. (St. Louis, MO, USA). Ryanodine and adenosine-5'-(β,γ -methylene)-triphosphate lithium (AMP-PCP) were purchased from Calbiochem (San Diego, CA, USA) and [³H]-ryanodine (82 Ci/mmol) was from Dupont, (Wilmington, DE, USA). Other chemicals used were of the best quality available.

Sarcoplasmic reticulum (SR) fraction

Heavy sarcoplasmic reticulum (SR) membrane fraction was isolated from fast twitch skeletal muscle from the back and hindlegs of 4-kg rabbits (New Zealand), according to Hamilton et al.¹² The RyR enriched fraction

collected at the 35–40% sucrose interface was suspended to a final concentration of about 50 $\mu\text{g}/\mu\text{L}$ in a buffer containing 10% sucrose, 0.1 M KCl, and 10 mM MOPS (pH 7.4), and stored at -70°C . Protein concentration was determined by the method of Lowry et al.,²⁹ using BSA as standard.

Radioligand binding studies

Equilibrium [^3H]-ryanodine binding was performed following the methodology described by Chu et al.⁹ Heavy SR membranes (10 μg) were incubated with 6 nM [^3H]-ryanodine for 12–14 h at room temperature in 0.25 mL of binding buffer containing 20 mM MOPS (pH 7.4), 300 mM KCl, 100 μM CaCl_2 , 100 $\mu\text{g}/\text{mL}$ bovine serum albumin, and variable concentrations of the modulators. When necessary, free calcium levels were adjusted in presence of 1 mM EGTA as calculated with the program CHELATOR.³⁰ Nonspecific binding was defined in the presence of 20 μM unlabeled ryanodine. Samples were filtered through Whatman GF/F glass fiber filters using a multifilter apparatus (Brandel, Gaithersburg, MD, USA). Filters were washed with five 5-mL aliquots of cold 300 mM KCl and counted in a scintillation spectrometer after the addition of 10 mL scintillation liquid (Tritonol).

Binding data analysis

The effect of calcium concentration on [^3H]-ryanodine binding in the presence or absence of compounds tested was analyzed applying the Hill equation. B_{max} and K_d were estimated directly from binding isotherms.³¹

[^3H]-Ryanodine association kinetics

The protocol followed was the reported previously by Chu et al.⁹ Briefly, heavy SR vesicles (100 μg of protein with ~ 15 pmol/mg of [^3H]-ryanodine binding sites) were added to [^3H]-ryanodine (7 nM), binding buffer, and 0.1 mg BSA, at room temperature, in 0.3 M KCl, 20 mM MOPS (pH 7.0), in the presence of the indicated modulators (see Fig. 1). At 15-min intervals, 300- μL aliquots were filtered, washed, and processed for radioactivity, as described above. Equilibrium values were obtained at 8 h. An association plot of $\ln \text{Beq}/(\text{Beq}-\text{B})$ versus time was analyzed, where Beq and B are the amounts of [^3H]-ryanodine bound at equilibrium and time t , respectively. The observed K_{+1} was derived from the slope. Association curves where the amount of [^3H]-ryanodine bound at equilibrium exceeded 5% of the [^3H]-ryanodine added were discarded.

Statistics

All results were expressed as mean \pm SEM. The significance of the differences among groups was assessed by two-way ANOVA test followed by a Tukey multiple comparisons post hoc test with α set at $p < 0.05$.

Dipole moment calculations

Dipole moments were calculated theoretically.^{32,33} A preliminary geometry of each purine derivative was

obtained using the molecular mechanics program PCMODEL 4.0 (Serena Software, Bloomington, IN, USA). The resulting geometries were optimized with the quantum mechanical, ab initio, all electron, restricted hartree-fock method, RHF, with the 6-31G* basis set. This level of theory has been found to predict quite accurately the experimental geometries and very reasonable charge distributions.^{32,33} The calculations were carried out with the program package PC GAMESS Ver. 6.1.^{34,35}

The calculated dipole vectors were visualized with the program package gOpenMol 2.1.³⁶ All molecules were aligned in the same way in the graph to facilitate the analysis.

All structures were calculated in their keto form, which is the predominant neutral tautomer at pH 7.^{21,22}

Combining the theoretical information derived from the calculations of dipole moments and the biochemical binding experiments for each purine, a QSAR was determined. The aim of this kind of analysis is to find a quantitative relationship between the activity of different related compounds with some of their structural features through a multiple regression analysis and an analysis of variance (ANOVA).³⁷ The analysis was performed with the programmed Microsoft Excel worksheet QSARDEMO built from the multilinear regression and ANOVA tool included in Microsoft Excel. The sheet is available upon request from the author, Dr. G. Höjer, Departamento de Física y Química Teórica, Facultad de Química. UNAM. Cd. Universitaria, 04510. México D.F.

Acknowledgements

The authors thank Drs. Ataulfo Martínez and Manuel Aguilar for their critical review of the manuscript. We are also grateful to Lic. in Nut. Fernando López-Barra and Biol. Olivia Vázquez-Martínez for helping to prepare the artistic design of the figures. This research was partially supported by a grant from DGAPA (IN 200-500). A.B.O. was a fellow from CONACyT and DGEP.

References and Notes

1. Fleisher, S.; Inui, M. *Annu. Rev. Biophys. Biophys. Chem.* **1989**, *18*, 333.
2. Rousseau, E.; LA Dine, Q; Meissner, G. *Arch. Biochem. Biophys.* **1988**, *15*, 75.
3. Smith, J.; Imagawa, T.; Ma, J.; Fill, M.; Campbell, K. P.; Coronado, R. *J. Gen. Physiol.* **1988**, *92*, 1.
4. Seryseva, I.; Schatz, M.; van Heel, M.; Chiu, W.; Hamilton, S. *Biophys. J.* **1999**, *77*, 1936.
5. Takeshima, H.; Nashimura, S.; Matsumoto, T.; Ishida, H.; Kangawa, K.; Minamino, N.; Matsuo, H.; Ueda, M.; Hanaoka, M.; Hirose, T.; Numa, S. *Nature* **1989**, *339*, 439.
6. Pessah, I.; Stambuk, R. A.; Casida, J. *Mol. Pharmacol.* **1987**, *31*, 232.

7. Holden, C. P.; Padua, R. A.; Geiger, J. D. *J. Neurochem.* **1996**, *67*, 574.
8. Morii, H.; Makinose, M. *Eur. J. Biochem.* **1992**, *205*, 979.
9. Chu, A.; Diaz-Muñoz, M.; Hawkes, M. J.; Brush, K.; Hamilton, S. L. *Mol. Pharmacol.* **1990**, *37*, 735.
10. Meissner, G. *J. Biol. Chem.* **1984**, *259*, 2365.
11. Chan, W. M.; Welch, W.; Sitsapesan, R. *Br. J. Pharmacol.* **2000**, *130*, 1618.
12. Hamilton, S. L.; Mejia, R.; Fill, M.; Hawkes, M. J.; Brush, K.; Schilling, W. P.; Stefani, E. *Anal. Biochem.* **1989**, *183*, 31.
13. Antaramián, A.; Butanda-Ochoa, A.; Vázquez-Martínez, O.; Vaca, L. *Cell Calcium* **2001**, *30*, 9.
14. Solomons, T. W. G. In *Organic Chemistry*; John Wiley and Sons: New York; p 39.
15. Hruska, S.; Danyluk, S. S. *J. Am. Chem. Soc.* **1968**, *90*, 3266.
16. Rao, S. T.; Sundaralingam, M. *J. Am. Chem. Soc.* **1970**, *92*, 4963.
17. Altona, C.; Sundaralingam, M. *J. Am. Chem. Soc.* **1972**, *94*, 8205.
18. Olsson, R. A. In *Proceedings of the International Symposium on Adenosine*; Berne, R. M., Rall, Th. W., Rubio, R., Eds.; Martinus Nijhoff: Charlottesville, VA, 1982; p 33.
19. Liu, S. S.; Yin, C. S.; Wang, L. S. *J. Chem. Inf. Comput. Sci.* **2002**, *42*, 749.
20. Rosseau, E.; Pinkos, J.; Saravia, D. *Can. J. Phys. Pharmacol.* **1992**, *70*, 394.
21. Chenon, M.Th.; Pugmire, R. J.; Grant, D. M.; Panzica, R. P.; Townsend, L. B. *J. Am. Chem. Soc.* **1975**, *97*, 4636.
22. Lange, N. A.; Dean, J. A. In *Lange's Handbook of Chemistry*; McGraw-Hill: New York, 1985, p 5.19.
23. Bhat, M. B.; Zhao, J.; Zang, W.; Balke, C. W.; Take-shima, H.; Wier, W. G.; Ma, J. *J. Gen. Physiol.* **1997**, *110*, 749.
24. Du, G. G.; Oyamada, H.; Khanna, V. K.; MacLennan, D. H. *Biochem. J.* **2001**, *360*, 97.
25. Knighton, D. R.; Zheng, J.; Eyck, L. F. T.; Ashford, V. A.; Xuong, N.; Taylor, S. S.; Sowadski, J. M. *Science* **1991**, *253*, 407.
26. Zarka, A.; Shoshan-Barmatz, V. *Eur. J. Biochem.* **1993**, *213*, 147.
27. Hadad, N.; Martin, C.; Ashley, R. H.; Shosan-Barmatz, V. *FEBS Lett.* **1999**, *455*, 251.
28. McGarry, S. J.; Williams, A. J. *J. Membr. Biol.* **1994**, *137*, 169177.
29. Lowry, O. H.; Rosenbrough, N. J.; Farr, A. L.; Randall, R. L. *J. Biol. Chem.* **1951**, *193*, 265.
30. Shoenmakers, T. J. M.; Visser, G. J.; Flik, G.; Theuvenet, A. P. R. *Biotechniques* **1992**, *12*, 870.
31. Weiland, G. A.; Molinoff, P. B. *Life Sci.* **1981**, *29*, 313.
32. Leach A. R. In *Molecular Modeling Principles and Applications*; Longman: Essex, 1996; p 595.
33. Jensen, F. In *Introduction to Computational Chemistry*; John Wiley and Sons: New York, 1999; p 429.
34. Schmidt, M. W.; Baldrige, K. K.; Boatz, J. A.; Elbert, S. T.; Gordon, M. S.; Jensen, J. J.; Kodeki, S.; Matsunaga, N.; Nguyen, K. A.; Su, S.; Windus, T. L.; Dupuis, M. *J. Comput. Chem.* **1993**, *14*, 1347.
35. Granovsky, A. A. <http://www.clasic.chem.msu.su/gran/games/index.html>
36. Laaksonen, L. <http://www.csc.fi/laaksonen/gopenmol/>
37. Hansch, C.; Fujita, T. *J. Am. Chem. Soc.* **1999**, *68*, 1616.